

Design and Fabrication of a Post-Buckled Amplification Mechanism to Actuate Trailing Edge Flaps for Helicopter Vibration Reduction

Rajnish Mallick¹, Ranjan Ganguli², M. Seetharama Bhat³

^{1,2,3} Department of Aerospace Engineering, Indian Institute of Science, Bangalore 560012, India

Abstract

One of the potential methods to alleviate helicopter vibration is use of on-blade active control trailing edge flaps (TEFs). The state-of-the-art smart actuators such as piezoelectric stack actuators are well suited for actuating full scale trailing edge flaps. Piezoelectric stack actuator (APA-500L) is used in this investigation as a prime mover. APA-500L can generate large forces in static and dynamic condition but is limited by small displacements. A linear amplification mechanism (LX-4) is devised to amplify the linear motion of the APA-500L actuator. A novel pinned-pinned post-buckled beam is used as a linear to rotary motion amplification mechanism (AM-2) to actuate the smart trailing edge flaps. The linear motion amplification mechanism (LX-4) is coupled with AM-2 to achieve the enhanced angular flap deflections. It is found that AM-2 can generate large angular TEF deflections of the order of 12 degrees in static test case. Aeroelastic analysis is also performed with AM-2 amplification mechanism and it leads to 91% vibration reduction from the baseline case. AM-2 has enormous potential for the rotorcraft community for actuating trailing edge flaps to realize various active control techniques such as helicopter vibration reduction and flaps for primary control. The paper also shows how both upwards and downwards motion of the flap can be obtained.

1. INTRODUCTION

Helicopter vibration alleviation is one of the most challenging problems faced by the rotorcraft community. Helicopters are subject to severe vibration levels because of the unsteady aerodynamic environment around the rotor^[1-2]. During the last two decades, researchers have developed various active techniques to suppress vibrations, such as, Higher Harmonic Control (HHC)^[3], Active twist rotor (ATR)^[4-5], Individual blade control (IBC)^[6], on blade partial span active trailing edge flaps^[7-8]. Smart materials such as piezoelectric stack actuators are ideally suited for actuating full scale trailing edge flaps (TEFs)^[9-11]. Piezoelectric stack actuators are light in weight, possess high energy density and contain less moving parts. Inherently, piezoelectric actuators have large force but generate small displacements. To actuate TEFs with suitably large angular deflections, a linear to rotary motion amplification mechanism is required. In the recent past, considerable effort has been devoted towards this endeavor. Lee and Chopra had developed an L-L lever fulcrum type amplification mechanism^[12]. They tested the L-L mechanism under centrifugal loading and an amplification factor

of around 21 was obtained. Hall and Prechtel devised an X-frame actuator driven by a piezoelectric material and tested it on a Mach scaled rotor system for various load cases^[13]. Most of the amplification designs available in literature are based on lever arm mechanisms. There is a scope for design and development of novel designs for amplification mechanisms, which are more efficient than the existing designs.

In this paper, we study the use of elastic buckling and dynamic instabilities for an amplification mechanism. Flexible rods can be used to deploy space antennas and control robotic motions. Some researchers have studied the post-buckling of an elastica rod with various end conditions. For example, beams with clamped-pinned boundary conditions^[14-15] and pinned-pinned end conditions^[16-17] have been considered. Holmes et al. investigated elastic buckling of an inextensible beam with hinged ends and fixed end displacements. They considered constrained Euler buckling and bifurcation analysis^[18]. Researchers have also studied buckling dynamics for development of novel mechanisms in several applications, such as, compliant mechanisms, UAV, morphing wings, MAV, etc.^[19].

¹ Ph.D. student, rajnish@aero.iisc.ernet.in

² Professor, ganguli@aero.iisc.ernet.in

³ Professor, msbdcl@aero.iisc.ernet.in

In this investigation, we evaluate and provide details of a novel linear-to-rotary motion amplification mechanism with pinned-pinned post-buckled beam (AM-2) to actuate trailing edge flaps. This paper builds on our previous paper^[17] and gives details of design and fabrication of the mechanism.

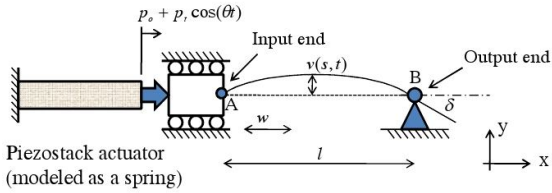


Figure 1. Schematic of the pinned-pinned buckled beam motion amplification mechanism

Figure 1 shows the schematic diagram of the pinned-pinned post-buckled beam with a piezostack actuator. APA-500L piezoelectric stack actuator (from CEDRAT Technologies, France) is used to actuate the mechanism.

2. EXPERIMENTAL SETUP

Physical and 3D computer-aided design models of the test setup are developed. CAD models are developed using CATIA-V5 for 660 mm and 150 mm long trailing edge flaps for push-pull lever arm mechanism (AM-1) and post-buckled mechanism (AM-2), respectively. These two mechanisms are discussed next.

A lever arm motion amplification mechanism (AM-1) developed here is shown in Figure 2. A T-shaped clevis is designed which is attached to the flap body through the flange of the clevis. A hinge is made at 15 mm from the base of the flap; effectively hinge is at 4mm from the axis of rotation (at the quarter chord). A separate hatch is cut out to allow easy access to the mechanism in the wing section as illustrated in Figure 2b.

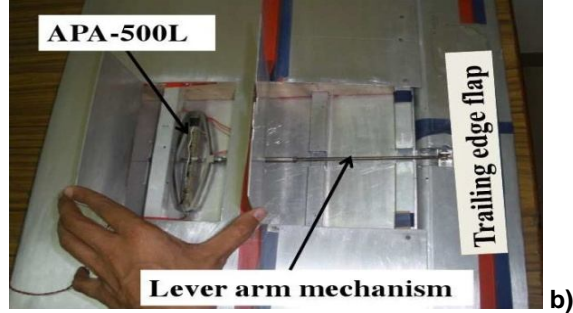
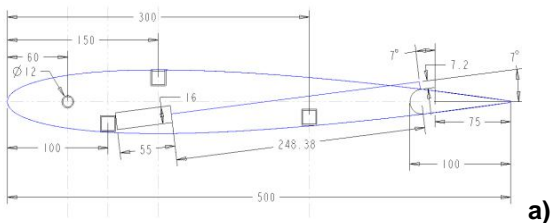
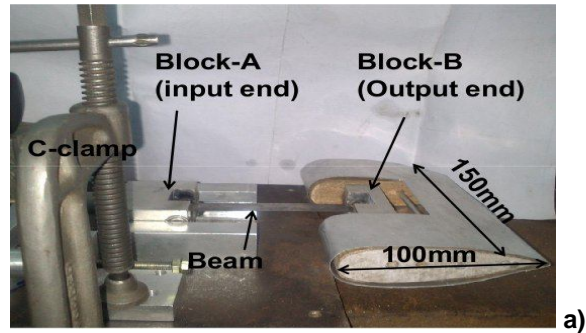


Figure 2. a) Drawing of rotor blade test section with AM-1 mechanism (Side view) b) Top view of the physical model of rotor blade test section with piezostack actuator and AM-1 inside the wing section, with hatch lifted.

Since 500µm linear displacement can be obtained from the piezostack actuator, AM-1 can generate maximum of ± 4 degree flap deflections. In the dynamic conditions, tip of TEF moves vertically by 10.5mm and hence the mechanical gain of AM-1 is 21. With this mechanical leverage, flap deflections are good enough in static case (non-rotating blade). As reported in literature, angular deflections decrease at least one order of magnitude for dynamic cases^[20-21]. Hence, to further amplify the flap deflections, a pinned-pinned post-buckled motion amplification mechanism called AM-2 is developed.

Here, AM-2 is shown in Figure 3. The NACA-0012 airfoil is selected for TEF cross-section profile. The flap has 150mm span and 100mm chord length. The beam dimensions are 80mm X 16mm X 0.5 mm and the beam is made of spring steel material. As shown in Figure 3, block-A is axially compressed by about 0.25mm, which is the available displacement of the piezostack actuator (APA-500L) for input voltage of 80 Vp-p. In this case, we observe that the flap deflects by 2.5 degrees. To further amplify the flap angles, we need larger axial displacements.



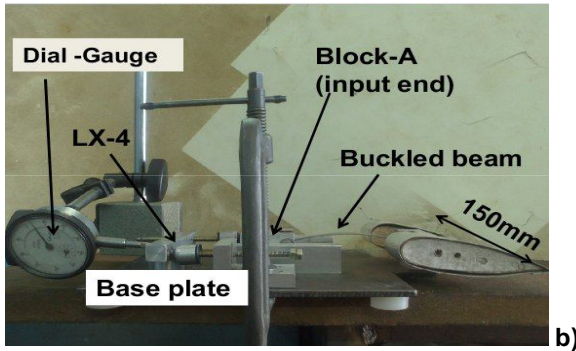


Figure 3. Fabricated prototype of the 150mm flap with pinned-pinned post-buckled beam (AM-2) **a)** Baseline case **b)** Post-buckled beam with deflected flap.

To obtain this goal, a linear amplification mechanism called LX-4 is designed and developed, which amplifies the axial motion from the piezostack by a factor of 4. The maximum available axial displacement from APA-500L is $500\mu\text{m}$ for peak-to-peak voltage input of 170V. Thus, with LX-4 we are able to amplify axial motion to $2000\mu\text{m}$ or 2mm. Here the LX-4 mechanism arms are made of spherical joints with a rolling point contact. This is essential for the desired amplification; otherwise the net force will be transferred to the rigid arms. There is a trade-off between force and displacement for amplification mechanism. As the displacement is increased by 4 times, the force decreases by a factor of 4. Piezostack actuator can generate maximum of 250N in dynamic condition. When LX-4 is used in conjunction with APA-500L actuator, the input axial compressive force available at input end-A, reduces to around 62N.

To ensure smooth buckling of the beam, beam dimensions are modified to reduce the Euler buckling load. Hence, the new beam dimensions are 97mm X 12mm X 0.5mm. Figure 3b shows the buckled beam mechanism with LX-4. In static condition, pinned-pinned post-buckled amplification mechanism coupled with LX-4 leads to enhanced flap deflections of the order of 12 degrees for 2mm linear motion of block-A as shown in Figure 10b.

To simulate the realistic case, both AM-1 and AM-2 mechanisms should deflect a full scale TEF by suitable angles. The mechanisms are tested with full scale TEF model. Design and fabrication of the wing section and TEF is discussed in the following section.

3. DESIGN OF WING SECTION AND TEF

A 3D CAD model of the wing section is developed using a 3D modeling package (Pro-E) with a trailing

edge flap. This exercise ensures that the final assembly of the flap and various components comprising a wing section along with a piezostack actuator works well in the physical model. Figure 4 shows the virtual model of the wing section with a trailing edge flap.

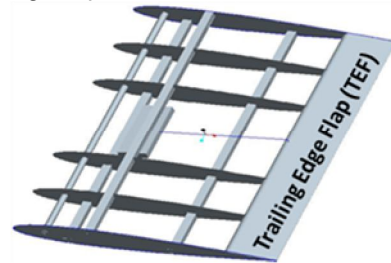


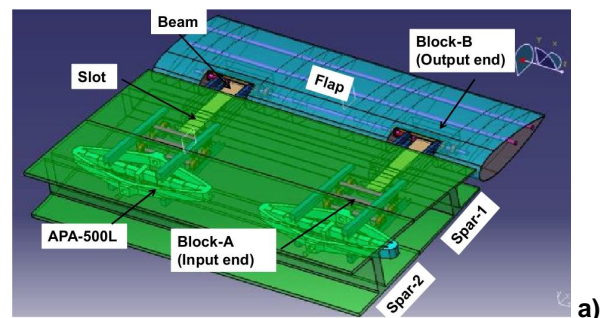
Figure 4. CAD model of wing section.

The wing section model used in this study is 660mm long and has 500mm chord length with a NACA 0012 (symmetric) airfoil cross-section made of aluminium. Ribs are made from balsa wood and 3 aluminium longerons are used to ensure the profile and strength of the wing section.



Figure 5. Side view of physical model of the wing section

A trailing edge flap with 20% chord length, is chosen as a representative of a TEF that could be analyzed as an oscillating control surface on rotor blade test section. The span of the flap is 660mm. Figure 5 shows fabricated wing section model with TEF. The motivation to choose this span length for TEF is from the observation that TEFs spanning 10%R when placed between 65%R to 85%R from the root for a full scale rotor blade leads to maximum vibration reduction^[22].



a)

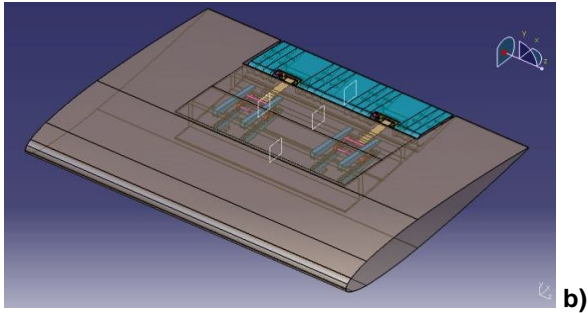


Figure 6. a) Dual AM-2 mechanism with TEF **b)** TEF with AM-2 inside the wing section.

Figure 6a shows TEF with dual AM-2 mechanisms. Here the block-B is attached to the spar-1 through 4 arched aluminum rods and block-A is placed in between the webs of spar-1 and spar-2 I-section. A slot is cut in the web of spar-1 to attach the buckled beam with block-B. Figure 6b shows the TEF inserted in the full scale wing section with AM-2 amplification mechanism assembly. Buckling of beam is essentially a bi-stable phenomenon. When block-A is compressed axially, beam buckles in a particular direction. Most of the test runs lead to beam hogging, which leads to downwards motion of the flap. Two new concepts are proposed to ensure both upward and downward motion of the TEF as required to suppress the helicopter vibrations or for primary control.

4. CONCEPTUAL DESIGN FOR ACTIVE BIASING FOR FLAP ROTATIONS

Figure 7 shows the conceptual design for active biasing using a disc cam mechanism. Figure 7a and 7c illustrate the undeflected flap configuration, denoted as R configuration. To ensure the downward motion of the flap, a soft spring is mounted on the base plate near the center of the beam. Spring top face touches the beam and creates an initial imperfection which results in positive rotation of the flap (+R configuration) as shown in Figure 7b. For upward motion of the flap, a disc cam is used which pushes the beam center downward. A stepper motor is used to drive the disc cam. When input block-A is compressed, then the imperfection in beam created by the disc cam results in a negative rotation of flap (-R configuration), as illustrated in Figure 7d. The active biasing can be achieved by adjusting the stepper motor frequency to be equal to the desired flap frequency. Note that the input frequency of the piezostack actuator is double the targeted flap frequency as shown in Figure 8.

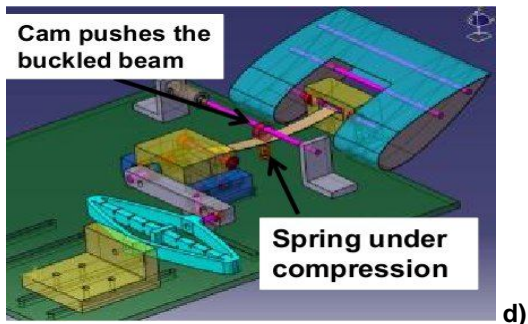
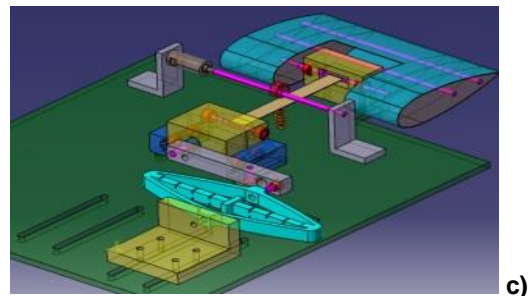
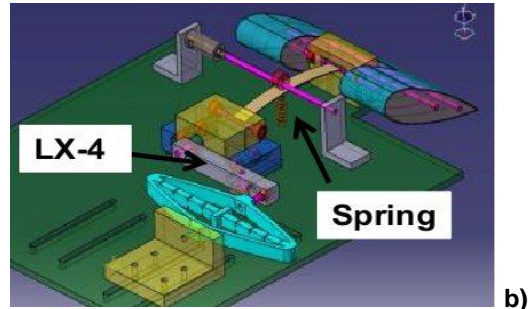
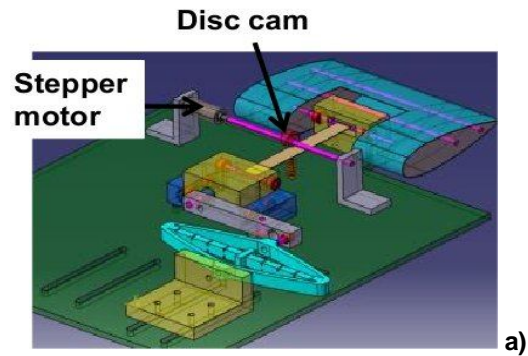


Figure 7. Concept:1, a) R configuration **b)** +R configuration **c)** R configuration **d)** -R configuration with cam design.

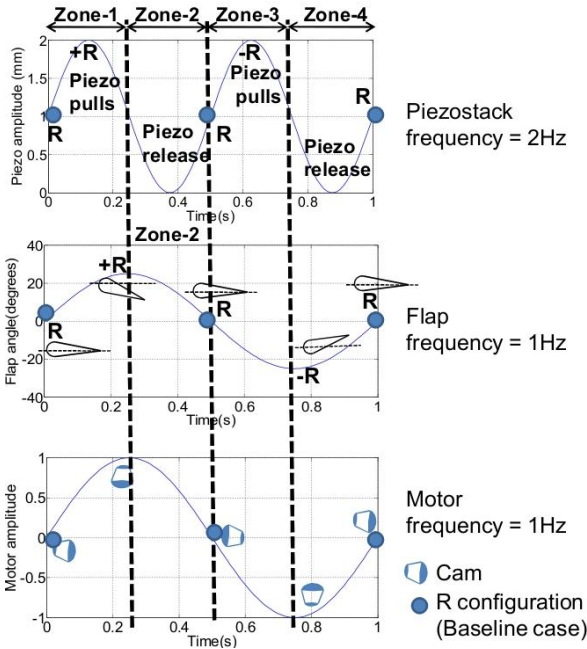


Figure 8. Piezostack actuator, flap and stepper motor signals for active biasing.

The description of the active biasing technique is summarized in Table 1.

Table 1. Summary of the operation of various devices for active biasing

Piezo Signal	Zone-1	Zone-2	Zone-3	Zone-4
Piezo	Pulls LX-4	Pushes LX-4	Pulls LX-4	Pushes LX-4
LX-4	LX-4 pushes block-A	LX-4 pull block-A	LX-4 pushes block-A	LX-4 pull block-A
Spring	Creates positive curvature	Creates positive curvature	Under Compression	Slowly coming back to original shape
Beam	Generate +R	Coming back to R	Generate -R	Coming back to R
Cam	Out of contact of beam	Starts grazing the beam	In contact, pushes beam	Slowly Starts leaving contact

Similarly in concept 2, shown in Figure 9, a solenoid switch is proposed replacing the stepper motor and cam. The conceptual design for R to +R configuration and R to -R configuration is illustrated in Figure 9.

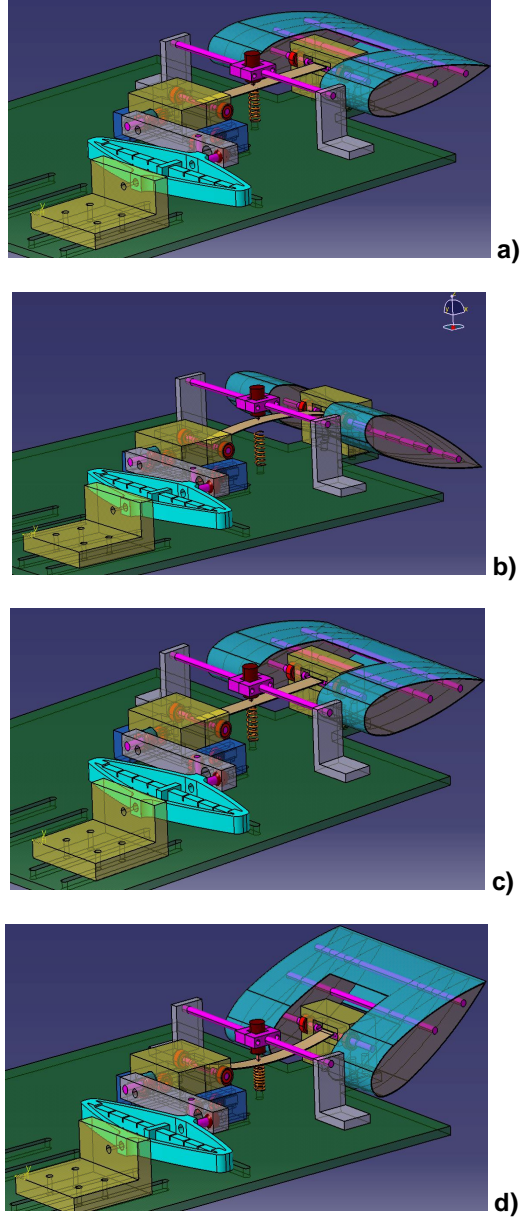


Figure 9. Concept:2, a) R configuration b) +R configuration c) R configuration d) -R configuration with solenoid design.

Researchers have used dual piezostack configurations to create active moments by switching the signals^[23]. The advantage of using above designs for active biasing of flap is that we can use only one piezostack actuator, which is the most

expensive component. The achieved flap rotations are adequate for TEF deflections to alleviate the helicopter vibrations. The AM-2 mechanism is cascaded with the aeroelastic analysis and hub loads are analyzed. Helicopter model used in the aeroelastic analysis is described in the following section.

5. AEROELASTIC ANALYSIS

In the aeroelastic analysis, the helicopter is represented by a nonlinear model of several elastic rotor blades, dynamically coupled to a six-degree-of-freedom rigid fuselage. Each blade undergoes flap bending, lag bending, elastic twist and axial displacement. Formulation is based on the generalized Hamilton's principle applicable to non-conservative systems.

$$(1) \quad \int_{\psi_1}^{\psi_2} (\delta U - \delta T - \delta W) d\psi = 0$$

Here δU , δT and δW are the virtual strain energy, kinetic energy and work, respectively. Finite element methodology is used to discretize the governing equations of motion. Unsteady aerodynamic models are used to predict the air loads due to blade and trailing edge flap motion^[24]. The resulting nonlinear ODEs in time are transformed into the normal mode space and solved for the steady-state blade response using the finite element in time procedure. The key finite element equation after normal mode transformation is:

$$(2) \quad M\ddot{p}(\psi) + C\dot{p}(\psi) + Kp(\psi) - F(p, \dot{p}, \psi) = 0$$

Here M , C and K are the normal mode mass matrix, damping matrix and stiffness matrix, respectively. Also, F is the force vector and p represents the modal displacement vector. ψ is the blade azimuth angle. Once the steady state blade response is determined, the loads acting at the rotor hub are calculated by summing the contributions of individual blades at the root. Thereafter, the helicopter is trimmed through a coupled trim procedure to find the blade response, pilot input control angles Θ and orientation of the vehicle, simultaneously. The coupled trim equation is:

$$(3) \quad F(\Theta) = 0$$

For a N_b bladed helicopter rotor with identical blades, the dominant component of hub vibratory loads is the $N_b\Omega$ harmonic, which is transmitted to the airframe. The details of the aeroelastic model are given in reference^[25]. This aeroelastic model has

been validated with wind tunnel data^[26] and flight test data^[27].

6. CONTROL ALGORITHM

The trailing-edge flap is deflected at higher harmonics of the rotor rotational speed. Typically, for a four-bladed rotor, the flaps are deflected at 3, 4 and 5/rev harmonics of the rotor rotational speed. The control law for the TEF can be written as:

$$(4) \quad \begin{aligned} \delta(\psi) = & \delta^{3c} \cos(3\psi) + \delta^{3s} \sin(3\psi) + \\ & \delta^{4c} \cos(4\psi) + \delta^{4s} \sin(4\psi) + \\ & \delta^{5c} \cos(5\psi) + \delta^{5s} \sin(5\psi) \end{aligned}$$

The six unknown flap harmonics in the above equation are determined based on an optimal control algorithm which minimizes a scalar objective function that is a quadratic function of the 4/rev hub vibratory loads (Z) and flap control harmonics (u).

$$(5) \quad J_v = Z^T W_z Z + u^T W_u u$$

The first term in the above equation is a scalar quantity relating purely to the hub vibration levels. The second term in equation (5) is introduced to keep the required control input (flap control angles) within practically achievable limits. In this study, the weighting matrix W_u is adjusted to limit the peak deflections of the flap which can be achieved using the current state-of-the-art smart materials. Z is the hub vibratory load vector containing the N_b / rev sine and cosine harmonics (three hub forces and three hub moments).

$$(6) \quad Z = [F_{xH}^{4P} \quad F_{yH}^{4P} \quad F_{zH}^{4P} \quad M_{xH}^{4P} \quad M_{yH}^{4P} \quad M_{zH}^{4P}]^T$$

$$(7) \quad u = [\delta^{3c} \quad \delta^{3s} \quad \delta^{4c} \quad \delta^{4s} \quad \delta^{5c} \quad \delta^{5s}]^T$$

The weighting matrix W_z is usually a diagonal matrix which can be suitably modified to make the controller reduce either the hub shears or moments. In the current study, all hub shears and moments are weighted equally. A global controller is used to determine the optimal control input^[28].

7. RESULTS AND DISCUSSION

In this section, experimental and numerical results are discussed for AM-1 and AM-2 mechanisms. The linear motion amplification mechanism (LX-4) generates around 2mm of linear stroke. LX-4 is cascaded with linear-to-rotary motion amplification mechanism (AM-2) and is tested under static conditions for various axial displacements. Figure

10a shows the undeflected flap position and Figure 10b illustrates the post-buckled beam induced flap deflections. The maximum flap angle observed in static case with LX-4 is 12 degrees for 2mm axial displacement of block-A as shown in Figure 10b.

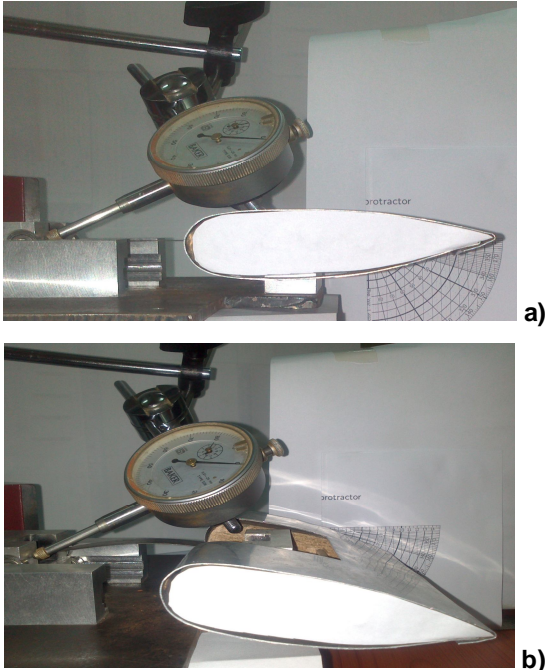


Figure 10. Trailing edge flap deflections with AM-2 for static case **a)** straight beam **b)** Post-buckled beam.

The different amplification mechanisms developed for actuating TEFs are compared in static or in quasi-static case for flap angles and axial stroke lengths as shown in Figure 11. It can be observed that AM-2 post-buckled mechanism coupled with LX-4 comes out as the best candidate. The static flap deflections are recorded using a high-performance Inertial Measurement Unit (IMU) and Attitude Heading Reference System (AHRS), VN-100 Rugged (from VectorNav Technologies, USA) as shown in Figure 12. The detailed comparison of various other parameters is shown in Table 2. The AM-2 with LX-4 approach is well suited for primary control applications, in addition to vibration and noise control.

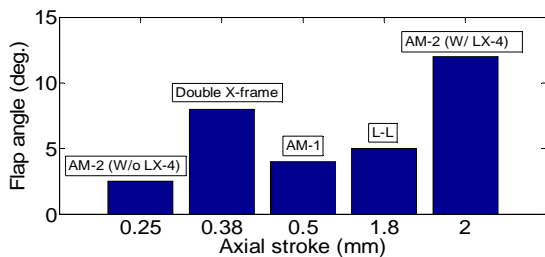


Figure 11. Flap angle and axial stroke comparison of various mechanisms to actuate TEF.

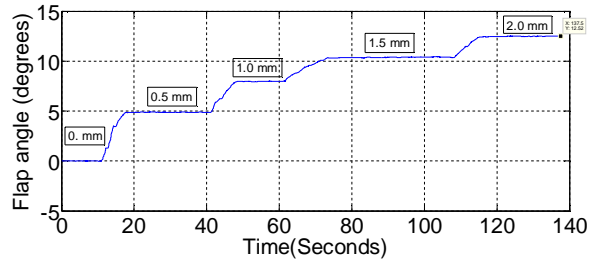


Figure 12. Flap angles for AM-2 with LX-4.

A computational study was also performed for vibration reduction in helicopter using on-board partial span trailing edge flaps at high speed forward flight $\mu = 0.3$. Using multi-harmonic inputs with AM-2 mechanism along with constant control weighting parameter, a reduction of 91% in hub load vibrations is observed, while 71% vibration reduction is observed with AM-1 mechanism. Thus, the post-buckling based mechanism is very promising.

Table 2. Comparison of various parameters among TEF actuation mechanisms

Mechanism Parameters	X-frame [13]	L-L [12]	AM-1	AM-2 w/o Lx-4	AM-2 w/ Lx-4
Amplification factor	15.2	21	21	6.6 (13.1)	31
Smart material	Piezo	Piezo	Piezo	Piezo	Piezo
Flap angle(deg.)	8	5	4	2.5 (5)	12
Axial stroke(mm)	0.38	1.8	0.5	0.25 (0.5)	2
Peak-to-peak voltage (V)	400	144	170	80 (170)	170
No. of Piezo stacks used	2	5	1	1	1

8. CONCLUSIONS

A pinned-pinned post-buckled beam motion amplification mechanism is designed and fabricated to actuate the trailing edge flap for helicopter vibration alleviation. Piezostack actuator (APA-500L) is used as the prime mover. It is found that the AM-1 lever fulcrum mechanism can generate maximum of

± 4 degrees of TEF deflections with 500 μ m of piezostack displacement. The AM-2 mechanism shows maximum flap deflection of 12 degrees for 2mm of axial motion of block-A at the input end of the buckled beam. A new design for linear motion amplification mechanism (LX-4) is developed and fabricated, which amplifies the linear stroke of piezostack actuator by factor of 4. The AM-2 mechanism, when coupled with LX-4, comes out as a potential solution for linear-to-rotary motion amplification mechanism for actuating trailing edge flap to suppress the helicopter vibrations up to 90%. Higher flap deflections from AM-2 mechanism shows its potential to be used for TEF actuation for helicopter rotor primary control which can lead to a swashplateless rotor^[29-30].

REFERENCES

- [1] P. P. Friedmann, M. De. Terlizzi, and T. F. Myrtle, "New developments in vibration reduction with actively controlled trailing edge flaps", *Mathematical and Computer Modelling*, Vol. 33, No. 10-11, 2001, pp. 1055-1083.
- [2] J. P. Narkiewicz, and G. T. S. Done, "A smart internal vibration suppressor for a helicopter blade - A feasibility study", *Journal of Sound and Vibration*, Vol. 215, No. 2, 1998, pp. 211-229.
- [3] S. R. Hall and N. M. Wereley, "Performance of higher harmonic control algorithms for helicopter vibration reduction", *Journal of Guidance, Control, and Dynamics*, Vol. 16, No.4, 1993, pp. 793-797.
- [4] M. Wilbur, P. Mirick, W. Yeager, C. Langston, C. Cesnik and S. Shin, "Vibratory loads reduction testing of the NASA/Army/MIT Active twist rotor", *Journal of the American Helicopter Society*, Vol. 47, No.2, 2002, pp. 123-133.
- [5] P. M. Pawar, S. N. Jung, "Active twist control methodology for vibration reduction of a helicopter with dissimilar rotor system", *Smart Materials and Structures*, Vol. 18, No. 3, 2009.
- [6] F. Nitzsche and E. J. Breitbach, "Using adaptive structures to attenuate rotary wing aeroelastic response," *Journal of Aircraft*, Vol. 31, No.5, 1994, pp. 1178-1188.
- [7] O. Dieterich, B. Enenkl and D. Roth, "Trailing edge flaps for active rotor control- Aeroelastic characteristics of the ADASYS rotor system", *In Proceedings of 62nd Annual Forum of the American Helicopter Society*, Phoenix, AZ, USA, 2006.
- [8] I. G. Lim and I. Lee, "Aeroelastic analysis of rotor systems using trailing edge flaps". *Journal of Sound and vibration*, Vol. 321, No. 3-5, 2009, pp. 525-536.
- [9] P. Leconte and H. M. des. Rochettes, "Experimental assessment of an active flap device", *In Proceedings of the AHS 58th Annual Forum of the American Helicopter Society*, Montreal, Canada, 2002.
- [10] R. Mallick, R. Ganguli and M. S. Bhat, "An experimental and numerical study of piezoceramic actuator hysteresis in helicopter vibration control using trailing edge flaps", *Journal of Aerospace: Part G*, DOI: 10.1177/0954410013478254, 2013.
- [11] S. Shevtsov, I. Zhilyaev, M. Flek, "GA based optimization of flextensional piezoelectric actuator for rotorcraft active vibration control", *In Proceedings of the 5th IMEF conference*, Prague, Czech Republic, 20-22 June, 2012.
- [12] T. Lee and I. Chopra, "Design of piezostack-driven tailing-edge flap actuator for helicopter rotors", *Smart Materials and Structures*, Vol. 10, No. 1, 2001, pp. 15-24.
- [13] S. R. Hall and E. F. Prechtel, "Development of a piezoelectric servo flap for helicopter rotor control", *Smart Materials and Structures*, Vol. 5, No. 1, 1996, pp. 26-34.
- [14] C. Y. Wang, "Post-buckling of a clamped simply supported Elastica", *International Journal of Non-Linear Mechanics*, Vol. 32, No.6, 1997, pp. 1115-1122.
- [15] J. Jiang and E. Mockensturm, "A motion amplifier using an axially driven buckling beam I: Design and experiments", *Nonlinear Dynamics*, Vol. 43, No.4, 2006, pp. 391-409.
- [16] U. Sonmez, "Buckling dynamics of imperfect elastica subject to various loading conditions", *International Journal of Mechanics and Materials in Design*, Vol. 3, No.4, 2006, pp. 347-360.
- [17] R. Mallick, R. Ganguli and M. S. Bhat, "Nonlinear dynamics of a post-bucked beam for actuating helicopter trailing edge flap", *In Proceedings of the 69th Annual forum of the American Helicopter Society*, Phoenix, Arizona, 21-23 May 2013.
- [18] P. Holmes, G. Domokos, J. Schmitt and I. Szeberenyi, "Constrained Euler buckling: an interplay of computation and analysis", *Computer Methods in Applied Mechanics and Engineering*, Vol. 170, No. 3-4, 1999, pp. 175-207.
- [19] R. Vos and R. Barrett, "Dynamic elastic-axis shifting: An important enhancement of piezoelectric postbuckled precompressed actuators", *AIAA Journal*, Vol. 48, No. 3, 2010, pp. 583-590.
- [20] J.-S. Kim, K. W. Wang, and E. C. Smith, "Synthesis and control of piezoelectric resonant actuation systems with buckling-beam motion amplifier", *AIAA Journal*, Vol. 46, No. 3, 2008, pp. 787-791.

- [21] A. A. Kumar, S. R. Viswamurthy and R. Ganguli, "Correlation of helicopter rotor aeroelastic response with HART-II wind tunnel test data", *In Proceedings of the 34th European Rotorcraft Forum*, Liverpool, UK, 16-19 September 2008.
- [22] S. R. Viswamurthy and R. Ganguli, "Optimal placement of piezoelectric actuated trailing-edge flaps for helicopter vibration control", *Journal of Aircraft*, Vol. 26, No. 1, 2009, pp. 244-253.
- [23] J. T. Szefi, E. Mockensturm, E. C. Smith, K.-W. Wang, P. Rehrig, L. Centolanza, "Development of a novel high authority piezoelectric actuator for rotor blades with trailing edge flaps", *In Proceedings of the 62nd Annual forum of the American Helicopter Society*, Phoenix, Arizona, May 9-11, 2006.
- [24] N. Hariharan and J. G. Leishman, "Unsteady aerodynamics of a flapped airfoil in subsonic flow by indicial concepts", *Journal of Aircraft*, Vol. 33, No. 5, 1996, pp. 855-868.
- [25] G. Bir, I. Chopra, R. Ganguli, E. Smith, J. Wang, K. Kim, W. Chan, M. Nixon, N. Kimata, and K. Nguyen, "University of Maryland advanced rotorcraft code (UMARC) manual", UM-AERO Report, 1994.
- [26] R. Ganguli, I. Chopra and W. H. Weller, "Comparison of calculated vibratory rotor hub loads with experimental data", *Journal of the American Helicopter Society*, Vol. 43, No.4, 1998, pp. 312- 318.
- [27] M. S. Torok and I. Chopra, "Rotor loads prediction utilizing a coupled aeroelastic analysis with refined aerodynamic modeling", *Journal of the American Helicopter Society*, Vol. 36, No. 1, 1991, pp. 58-67.
- [28] W. Johnson, "Self-tuning regulators for multicyclic control of helicopter vibration". *NASA Technical Paper*, 1996.
- [29] R. Ganguli, B. Jehnert, J. Wolfram, P. Vörsmann, "Optimal Location of Centre of Gravity for Swashplateless Helicopter UAV and MAV", *Aerospace Engineering and Aircraft Technology*, Vol. 79, No. 4, 2007, pp. 335-345.
- [30] R. Ganguli, B. Jehnert, J. Wolfram, P. Vörsmann, "Survivability of Helicopter with Individual Blade Primary Control Failure", *Aeronautical Journal*, Vol. 111, No. 1124, 2007, pp. 645-657.

Copyright Statement

The authors confirm that they, and/or their company or organization, hold copyright on all of the original material included in this paper. The authors also confirm that they have obtained permission, from the copyright holder of any third party material included in this paper, to publish it as part of their paper. The authors confirm that they give permission, or have obtained permission from the copyright holder of this paper, for the publication and distribution of this paper as part of the ERF2013 proceedings or as individual offprints from the proceedings and for inclusion in a freely accessible web-based repository.